DYNAMIC TESTING OF REINFORCEMENT SYSTEMS

John Player, Alan Thompson and Ernesto Villaescusa
Western Australian School of Mines
Curtin University of Technology,
Locked Bag 22, Kalgoorlie Western Australia 6433

ABSTRACT

The Rock Mechanics Group at the Western Australian School of Mines (WASM) in Kalgoorlie commenced development, design and construction of a unique dynamic testing facility in 2002. The facility is designed to quantify the force-displacement responses of reinforcement systems subjected to dynamic loading. Full scale reinforcement systems are tested with a double embedment configuration to simulate the load transfer action of in situ reinforcement. The facility uses a momentum transfer mechanism. The specimen is dropped on to a reaction surface to rapidly decelerate the reinforcement anchor length while the momentum of a large mass loads the collar of the reinforcement. This test method is quite different from previous testing methods. Evaluation of the results from a two year program of commissioning and processing of data were promising. The facility and the method of data analysis are described in detail by Player et al. (2004) and Thompson et al. (2004). The facility was recognized as the most advanced mining dynamic test facility for reinforcement systems at the time by Brown (2004).

A systematic program of testing of different reinforcement systems has been undertaken since 2004. Potentiometers, load cells, accelerometers and high speed video are used to monitor the tests. Software has been developed to analyse the data. The results from the analyses are presented in the form of displacement, velocity, acceleration and force variations with time for all components involved in a test and a force-displacement response and energy absorption capacity for the reinforcement system. The results from the testing program have resulted in the compilation of a database of force-displacement responses to different dynamic loading conditions. The results from a number of the reinforcement systems tested are presented and discussed. Assessments are made in regard to the likely effectiveness of these reinforcement systems when subjected to dynamic loading resulting from the violent failure of overstressed rock.

1.0 DYNAMIC TESTING OF REINFORCEMENT SYSTEMS

The WASM Dynamic Test Facility was purpose built to test reinforcement systems, support elements, and their combinations under dynamic loading conditions. The results from the tests are used to assess dynamic force-displacement responses and the energy consumed by the sample during the test. Elements such as cone bolts, cable bolt strand and threadbar were encapsulated with cement grout contained within thick wall steel pipes. Other systems that are sensitive to the mechanical installation (e.g. jumbo installed resin bolts) or the borehole conditions (e.g. friction stabilisers) were driven by a jumbo into simulated bore holes with a rough internal layer.

1.1 Dynamic loading mechanism

A potential may exist for dynamic ejection of failed material when a seismic wave encounters an excavation, see Figure 1. The potential depends on the energy in the wave (e.g. radiated energy and seismic moment), seismic source parametres (e.g. stress drop, corner frequency, and source radius), and site characteristics of the excavation (e.g. degree of fracturing, stored strain energy, and rock properties). The installed ground support (dynamic or non-dynamic capable) only acts to control the rock behaviour after failure; it does not prevent dynamical induced failure from occurring.

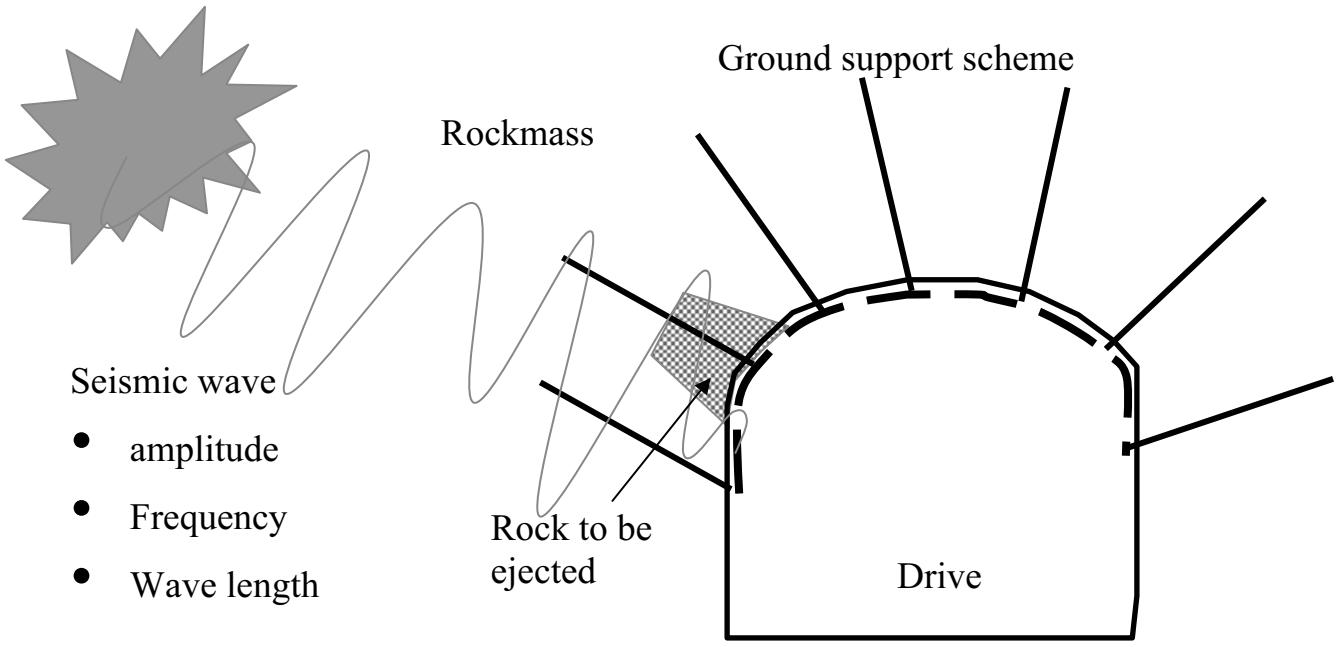

Figure 1 : Seismic Loading

A block of rock could be ejected or fragmented from the surrounding rockmass into the excavation following the encounter of a seismic wave with a susceptible excavation. This detachment process is unlikely to be instantaneous, but rather very quick. It will be related to the seismic wave velocity, amplitude and frequency and / or fracture growth velocity within the rockmass. The non-instantaneous process is suggested because the excitation source is a wave that has velocity, frequency and wave length. Instantaneous and very quick are defined in the context of the data acquisition system at the WASM Dynamic Test Facility. Instantaneous implies faster than the data acquisition rate, i.e. faster than 0.04 milliseconds, and very quick is defined as any time slower than the data acquisition rate.

1.2 Dynamic test facility

Figure 2 is a photo of the constructed facility with its primary components identified. The standard reinforcement test performed at the WASM Dynamic Test Facility uses an impact velocity of 6m/s and 2000kg of simulated ejected rock. A simulated discontinuity to allow double embedment testing was typically located 1.0m from the collar. This provides a nominal input of 36kJ of kinetic energy that must be absorbed by the reinforcement system.

Some of this energy and the energy of the beam must be absorbed by the buffers. The relative displacement of the mass compared to the drop beam following impact results in additional potential energy that the reinforcement system must be capable of absorbing; for high displacement capacity reinforcement systems this can be considerable. A schematic of the test sample and loading mass is shown in Figure 3. A critique of mining and civil dynamic testing facilities was published by Player, Villaescusa and Thompson (2005).

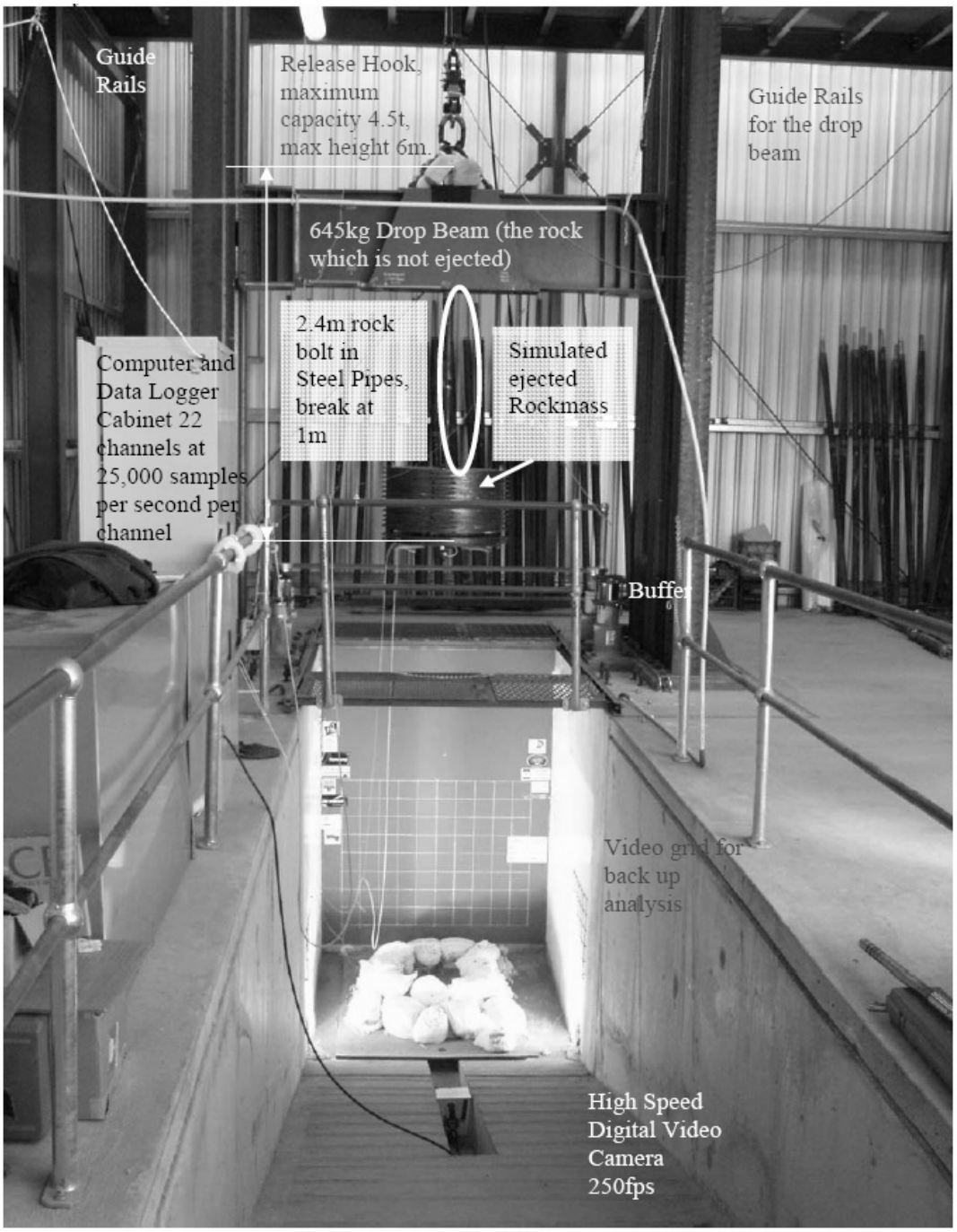

Figure 2 : WASM Dynamic Testing Facility

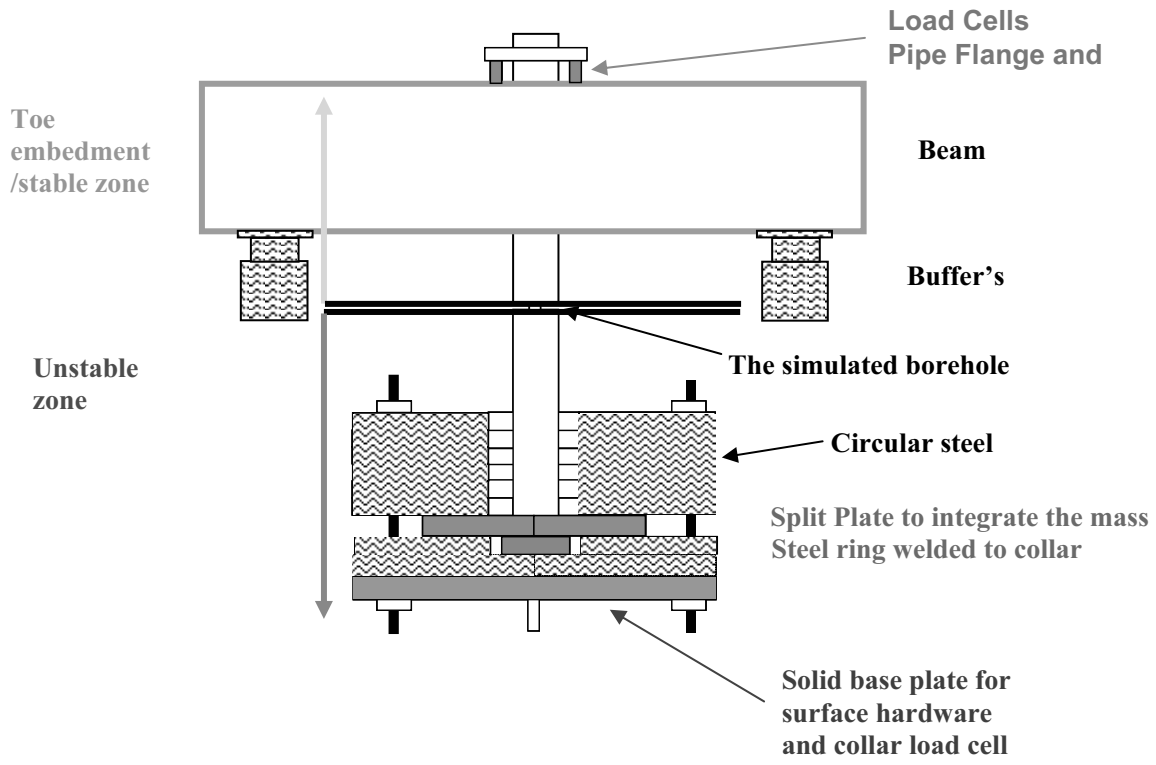

Figure 3 : Schematic of Test Sample and Loading Mass

1.3 Axial loading

The axial loading conditions simplify the test configuration and analysis process. Axial loading conditions are expected to provide an upper limit for most reinforcement systems tested; an exception may be friction stabilisers where shear loading is expected to increase the capacity from distortion of the split tube and partial locking into the borehole. A test program examining the dynamic properties of a reinforcement system in shear would need to be able to apply load at various angles to the axis of the element. The dynamic shear result must still be compared to dynamic axial loading results as they may represent the minimum or maximum performance of a reinforcement system.

1.4 Single versus multiple drops

Typically, the WASM analysis on a reinforcement system is based on the first drop, and provides the primary results. In practice a large seismic event that results in rockmass damage and a significant yielding of a reinforcement system would not be expected to sustain a similar subsequent loading event. In a situation where a second loading occurs, the loading mechanism to the reinforcement system would be quite different due to the fractured rockmass and changes to the embedment lengths.

To correctly evaluate the capacity of a reinforcement system in response to a single large dynamic event, a test facility must have sufficient energy to break the reinforcement system on the first impact and not rely on multiple impacts. Testing at the WASM Dynamic Test Facility has shown that multiple, non-critical loading results in a higher predicted capacity than when element failure results from a single large event. The WASM Dynamic Test Facility has up to 120kJ of input energy available for loading reinforcement systems to assess their upper limit.

1.5 Instrumentation and software

The instrumentation and software developed allow the calculation of the dynamic force-displacement response at the simulated discontinuity for the tested reinforcement system. The area under the force-displacement curve is the energy consumed by the reinforcement system in dissipating the input kinetic energy. It is possible for this dissipated energy to be greater than the input kinetic energy due to the change in potential energy of the loading mass following impact. The energy absorbed by the buffers is calculated for each test, the results show the buffers absorb the kinetic energy input from the drop beam.

The forces are calculated by multiplying mass by acceleration. The acceleration data are either the filtered deceleration response of accelerometers or calculated from the relative displacement of a target with a high speed digital video and derived from object tracking software.

The relative velocity between the drop beam and the loading mass is considered to be equivalent to the ejection velocity underground. A "block" of rock on the perimeter of a tunnel loaded by a dynamic event would initially be at rest relative to the surrounding rockmass. The complex ejection process occurs with the block being rapidly accelerated to a peak velocity and, then to rest if the reinforcement system does not fail. A "soft" reinforcement system will allow a higher ejection velocity and larger displacement for a particularly input velocity when compared to a "strong" reinforcement system. The amount of allowable deformation and whether the surface support has sufficient toughness to accommodate the deformation of the reinforcement system are key aspects that mining operations must consider.

Stable peak "ejection" velocities for the tested reinforcement systems vary between 2.2m/s and 3.8m/s for the 6m/s impact velocity tests. Reinforcement systems that have high resisting capacities and toughness result in high peak decelerations compared with low to moderate resistive capacity systems that allow large displacements to occur.

2.0 DYNAMIC TESTING PROGRAM REINFORCEMENT SYSTEMS

The WASM test program has examined the behaviour of a number of reinforcement system under dynamic loads. Those primarily examined are currently in use at Australian mining operations for the control of large ground deformations or dynamic loading conditions resulting from mine seismicity, or are being developed for that application. These include: plain strand cable bolts, fully encapsulated threadbar, debonded threadbar, cone bolts of various designs and encapsulation products, solid bolts with an internal yielding mechanism, friction stabilisers, and modified yielding cable. The first five will be discussed in detail. The reinforcement systems were grouted in September 2002 and tested between 2003 to 2007 unless otherwise stated.

A summary of the energy absorbed, dynamic forces, displacements and loading times for the various reinforcement systems will be discussed in Section 3.

2.1 15.2mm Plain Strand Cable Bolts

Single 15.2mm diameter plain steel strand cables were encapsulated with a 0.40 water-cement ratio into thick wall steel pipes. The pipes had a 76.3mm internal diameter and 101.9mm external diameter with an equivalent rockmass radial stiffness of 69GPa. (Hyett, Bawden and Reichardt, 1992). Each pipe was 2.58m in length with a simulated discontinuity located either 0.62m or 1.0m from the collar of the pipe. The strand has the static mechanical properties specified in Table 1.

Table 1: Physical and Static Mechanical Properties Single Strand Cable (Anon 2006)

	Minimum	Typical
Core Diameter (mm)		15.2
Cross Sectional Area (mm^2)		143
Yield Force 0.2% (kN)	212	235
Tensile Force (kN)	250	265
Elongation on 600mm length (%)	3.5	6.5

2.1.1 Testing Program

The plain strand cable bolts were tested with variations to the anchor and collar embedment lengths, surface hardware and loading velocity. The basic surface hardware consisted of a 200mm square 8mm thick bearing plate with a barrel and wedge anchor (item 1 in Table 2). The initial strand tension was 40-50kN. The following tables describes some of the tests and summaries their outcomes. They are listed in order of testing.

Table 2 is a summary of the cable bolt test program and Table 3 is a summary of the results.

Table 2: Summary of Plain Strand Cable Program

Bolt Number	Loading Mass (kg)	Impact Velocity (m/s)	Collar embedment (m)	Toe embedment (m)	Surface hardware	Comment
23	2030	5.95	1.0	1.58	1	Toe section slipped
27	2030	5.45	0.62	1.96	1	Snapped cable
22	2030	6.0	0.62	1.96	1 + rubber plate	Snapped cable, was retained for longer
19	2030	6.0	0.62	1.96	Nil	300mm of cable below collar, mass slides off
26	2030	5.8	1.0	1.58	Nil	300mm of cable below collar, mass slides significantly

Table 3 : Summary of Plain Strand Test Results

Bolt Number	Load Time (ms)	Displacement (mm)	Peak Deceleration (g)	Peak Force (kN)	Peak Ejection Velocity (m/s)	Energy Absorbed (kJ)	Results
23	73	73	-11	228	2.2	17	Stable toe slip
27	48	85	-14	302	2.8	18	Snapped cable
22	38	91	-12	254	3.75	18	Snapped cable
19	130	644	-3.0	78	5.5	34	Unstable mass slide off
26	288	650	-6	126	4.2	40	Unstable mass sliding

A higher loading velocity (8m/s at impact) was undertaken with a similar sample configuration to bolt 23. In this test the strand pulled completely out from the toe embedment. It is believed that the doubling of the input energy and possible grout embrittlement through aging prompted the cable to pull out completely rather then being restrained.

The mechanism for this failure is that at higher loading velocity the dynamic friction of the faster moving strand was too low to prevent pull out from occurring. Detailed explanation for the changes in bolt performance due to dynamic friction is explained in Section 2.5.5.

The bolt 27 configuration was repeated with the same result; snapped cable. An instrumentation issue with two of the tests did not allow full analysis and the partial results are presented.

2.1.1 15.2mm Plain Strand Cable Bolts Summary

Typical force-displacement responses for cable bolts that snapped, and cable bolts that slipped due to insufficient embedment length (collar and toe) are shown in Figure 4. Typical photos of these tests are shown in Figure 5.

The test work identified that plain strand cable bolt responses to strong dynamic loading conditions were highly dependent on the collar and toe embedment length and the use of surface hardware. A secondary dependency resulting from grout stiffness and loading velocity are suggested but not fully explored.

The dynamic axial loading conditions of the facility are most favorable to sliding of the strand through the cement grout. It would be difficult to design a short embedment to act as a sliding mechanism to strong ground motion due to the shear component that would also exist. The dynamic work interestingly confirmed static test work by Hutchins et al. (1990) that showed a plain strand cable does not generate sufficient load to break the cable with less than 2.0m of embedment.

Additional dynamic testing programs can be conducted to determine the reduced dynamic loading conditions that plain strand cable survives where the toe embedment is statically stable i.e. 2.0m embedment. Bulb strand cables are expected from static testing to have a lower deformation capacity then a plain strand cable with the same embedment length and hence be more prone to failure. Closer spaced bulbs will have less cable length available to dissipate the dynamic load prior to a non-moving stable condition being reached.

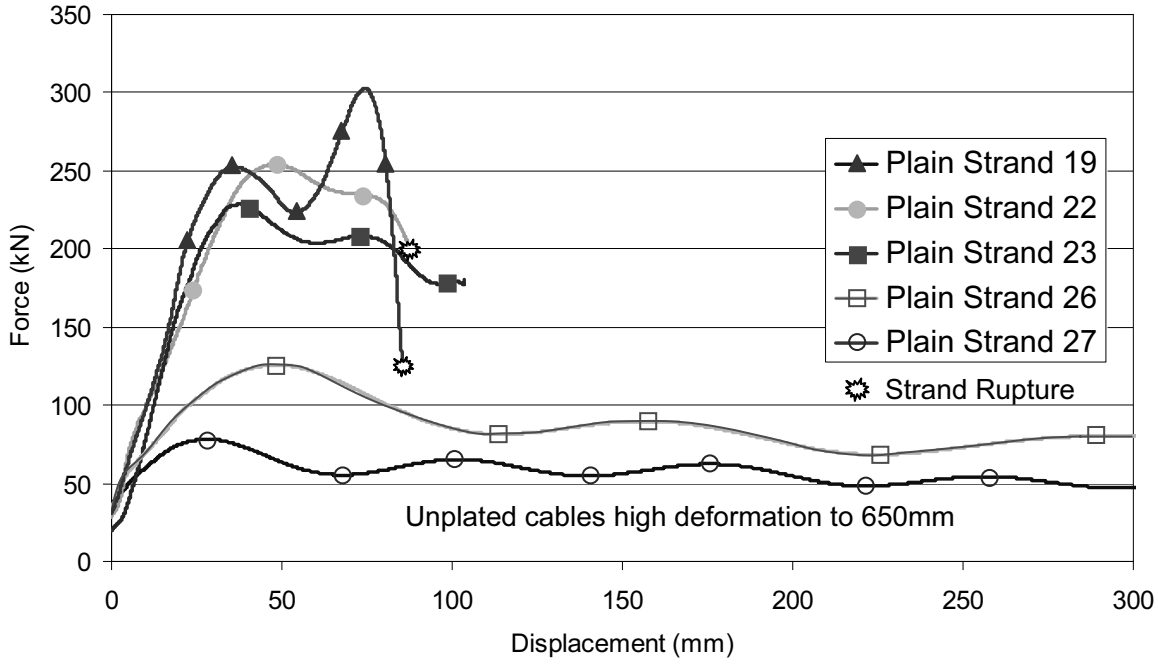

Figure 4: Dynamic force-displacement response for plain strand cable bolts

Figure 5 : Cable bolt test results – snapped strand first drop and a slipped strand first loading

2.2 Fully Encapsulated Threadbar

2.2.1 Testing Program

Dynamic loading has been applied to fully encapsulated 20mm diameter galvanised threadbar (10mm pitch coarse thread) of 2.4m total length. The collar embedment length was 1.0m and toe embedment length was typically 1.2 - 1.3m (depending on the amount of bar exposed at the collar). The thick wall steel pipe had 49.5mm internal diameter and 60mm external diameter and equivalent radial rock stiffness of 49GPa. Surface hardware consisted of a 150mm square 8mm thick dome plate, washer and separate nut.

The threadbar used (for fully encapsulated and debonded testing) had the reported static physical and mechanical properties given in Table 4.

Table 4: Static Mechanical Properties Threadbar (Anon 2006)

	Minimum	Average
Core Diameter (mm)	19.3	19.5
Cross Sectional Area (mm2)	293	299
Yield Strength (MPa)	500	550
Yield Force (kN)	147	165
Tensile Strength (MPa)	600	640
Tensile Force (kN)	175	191
Elongation (%)	12	21

The test program on the threadbar is detailed in Table 5 and the results are summarised in Table 6.

Table 5: Threadbar Test Program

Bolt Number	Loading Mass (kg)	Impact Velocity (m/s)	Input Energy (kJ)	Surface hardware	Comment
11	2020	4.8	23	yes	Bar streched
9	2020	5.95	36	yes	Bar fractured at simulated discontinuity
6	2020	5.8	34	yes	Bar fractured at simulated discontinuity
10	2020	5.85	35	no	Bar streched
5	1870	5.85	32	yes	Bar streched and pulled in grout, 5 year old grout

Table 6: Summary of Threadbar Test Result

Bolt Number	Load Time (ms)	Displacement (mm)	Peak Deceleration (g)	Peak Force (kN)	Peak Ejection Velocity (m/s)	Energy Absorbed (kJ)	Results
11	56	92	-12	248	2.2	14.8	Bar streched
9	26	62	-12	256	3.0	10.9	Bar fractured at simulated discontinuity
6	28	69	-12	260	3.1	13.9	Bar fractured at simulated discontinuity
10	56	100	-13	270	3.2	20.8	Bar streched
5	100	91	-13	235	2.4	17.5	Bar streched and pulled in grout, 5 year old grout

2.2.2 Summary Encapsulated Threadbar

Typical force-displacement responses for fully encapsulated threadbar are shown in Figure 6 and photos of example tests are in Figure 7. Both steel yield and fracture of the bar occurred at the simulated discontinuity.

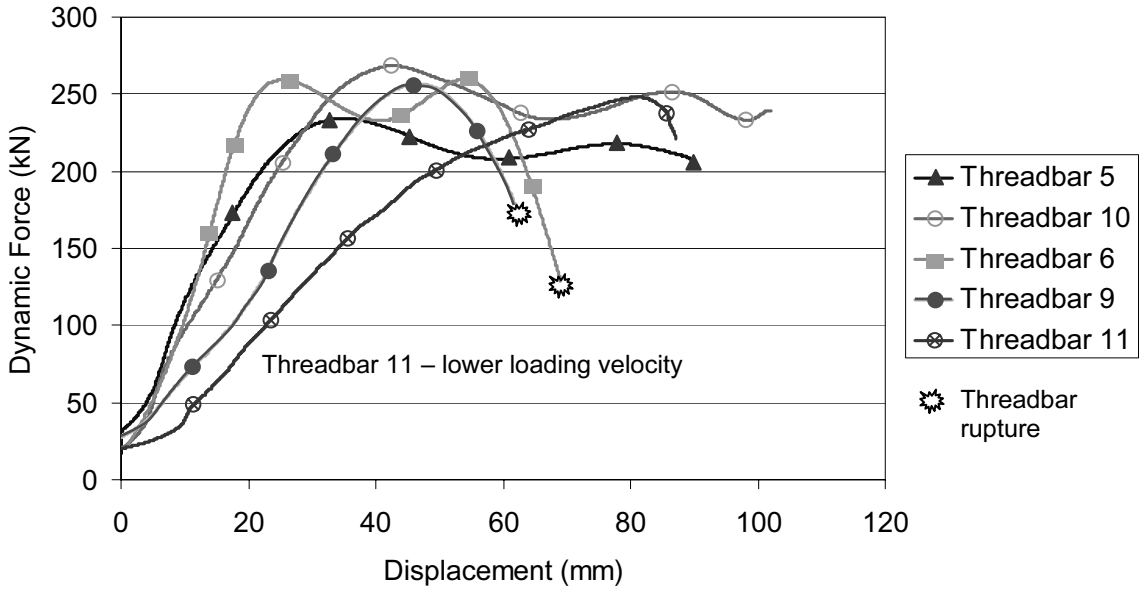

Figure 6: Dynamic force-displacement responses for fully encapsulated threadbar

Figure 7 : Threadbar results – snapped first loading and yield first loading

The encapsulated threadbar required plastic deformation of the steel bar at the simulated discontinuity to dissipate the input energy from the dynamic load. The dynamic axial loading conditions and partial threads of the bar allows the grout to interlock and the shaft to break under some critical loading conditions. The critical loading conditions are related to the rate at which the energy is consumed in the plastic deformation of the steel bar compared to the fracture growth between the steel bar and grout interface. At a sub-critical loading velocity the plastic deformation along the shaft of the bolt and the fracturing of the grout allows a free length to develop from the simulated discontinuity towards the toe and collar of the bolt. The fracture process fills the partial threads on the bolt with pulverised grout. This effectively reduces the embedment length towards the collar and toe increasing the central deformation length of the bolt.

This theory was validated by repeat testing on bolts 11 and 12 by starting at a subcritical loading state and then progressively increasing the loading velocities resulted in the toe of the bolting pulling out at an input energy greater than that used on bolts 6 or 9.

Under a shear loading state this process would be expected to alter as the frictional component would increase and most likely would promote failure of the bolt.

2.3 Debonded Threadbar

2.3.1 Testing Program

The debonded threadbar consisted of a 20mm diameter thread bar three metres in length. Debonding was provided by a plastic tube crimped to the central 1.6m of the bar, Figure 8. The bolts were encapsulated with a 0.4 water-cement ratio grout into thick wall steel pipe with an equivalent rock modulus of 49GPa, and tested after setting for one to two months. The program of four bolts assessed two different surface hardware attachments. The first two bolts (83 and 84) surface hardware used a separate nut and washer while the second two bolts (85 and 86) used an integrated nut and washer, Figure 9. All bolts were subjected to the standard WASM dynamic loading. Table 7 shows a summary of the results.

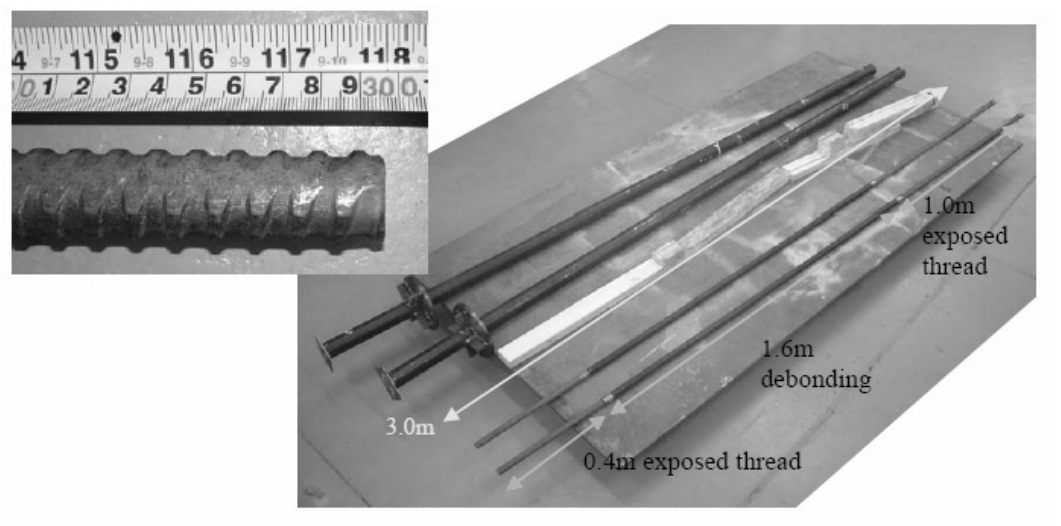

Figure 8: Debonded threadbar configuration

Figure 9: Separate nut and washer and the integrated nut and washer

Table 7: Summary of Debonded Threadbar Results

Bolt Number	Load Time (ms)	Displacement (mm)	Peak Deceleration (g)	Peak Force (kN)	Peak Ejection Velocity (m/s)	Energy Absorbed (kJ)	Results
83	55	93	-11.2	240	2.5	18	Nut stripped
84	35	82	-10.2	217	2.6	13.6	Nut stripped
85	58	101	-11.6	244	2.6	21.8	Reinforcement system survived two drops
86	62	106	-10.6	226	2.6	21.6	Reinforcement system partial thread shearing on second drop.

Published data on the performance of steel reinforcing bars under dynamic loads have increased yield points (both for elastic yield and ultimate plastic deformation yield point) which are dependent on the grade of the steel and the strain rate applied. Malvar and Crawford (1998) have shown for strain rates approximating one strain that per second the expected dynamic increase factor of approximately 1.3 for reinforcing bar of 550MPa yield stress. This increases the average yield load from 165kN to 213kN for the utilised threadbar; a result which is a good fit to the assessed dynamic yield load in Figure 10. The highly repeatable nature of the test facility was highlighted by testing this type of bolt which relies initially on elastic followed by plastic deformations of a steel bar.

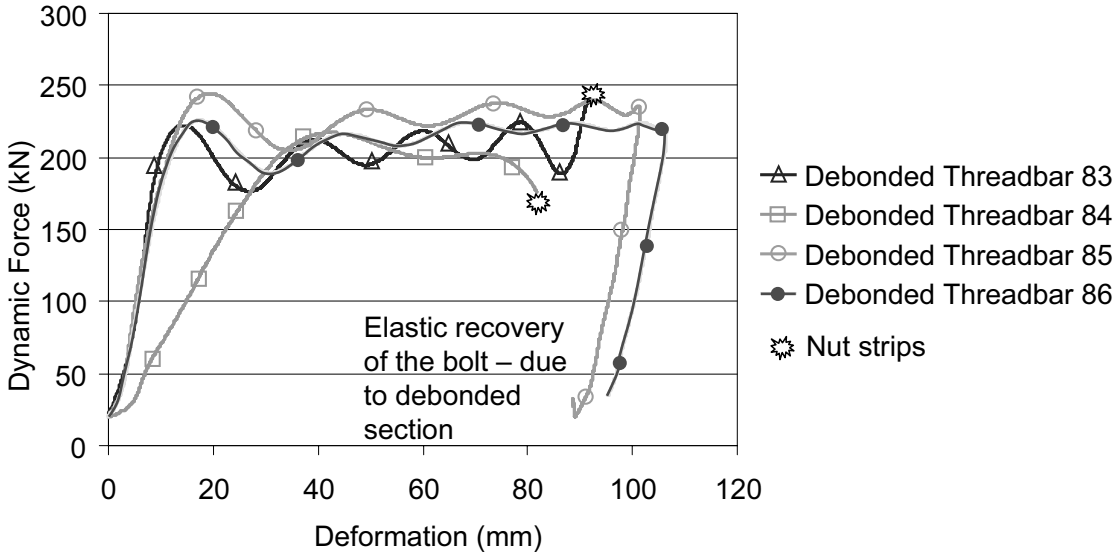

Figure 10: Dynamic force-displacement response for debonded threadbar

2.3.2 Summary Debonded Threadbar

The debonded threadbar required plastic deformation of the steel in the debonded length to absorb the input energy. To achieve this, the collar mass needed to transfer the load through the surface hardware and the side of the simulated bore hole onto the short length of encapsulated threadbar in the collar section.

The critical functionality for a debonded threadbar was the correct selection of the nut and washer to maximize the load transfer through the partial thread. The testing with separate nut and washer allowed the nut to be stripped over the threads on the first dynamic loading of the bolt at 180kN; but, when a longer integrated nut and washer were used, this increased to 200kN and the failure mechanism changed to either survival of the surface hardware or partial shearing of the threads along the shaft of the bolt, Figure 11. The load was measured by the collar load cell.

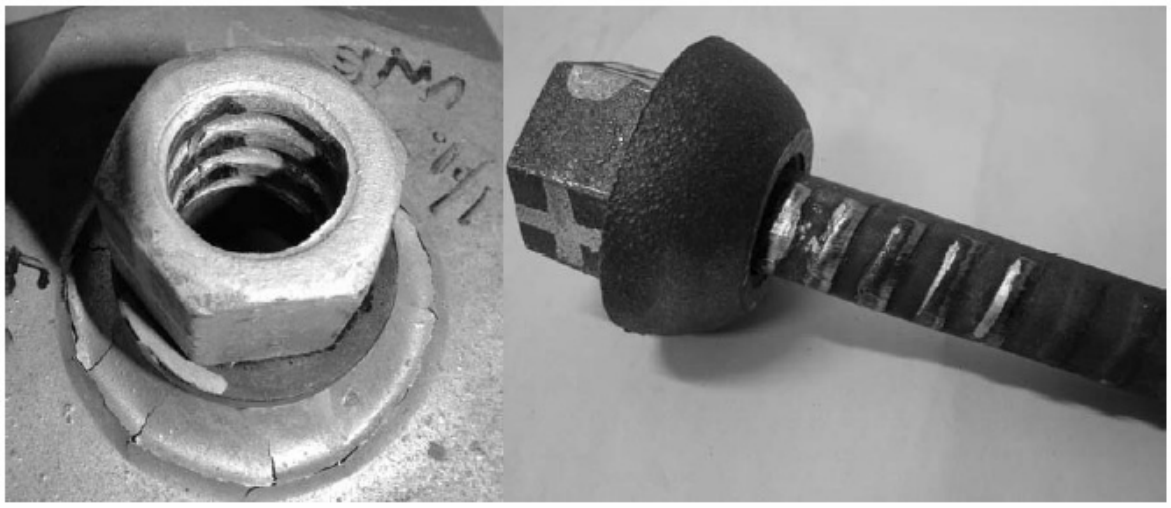

Figure 11 : Debonded threabar results - stripped nut and stripped thread

The second most important criterion appeared to be the collar embedment length; as the particular configuration of the test would always allow load to be transfered to the surface hardware.

Interestingly despite the shorter toe embedment length on these samples compared to the toe length of the 2.4m fully encapsulated bolts, there was no movement of the toe of the bolts. This suggests the grout fracturing and the development of an increase new "debonded" length is a lower order mechanism once a long debonded length has been established along the bolt.

2.4 22mm Cone Bolts

Dynamic loading of 22mm cone bolts with M24 threads encapsulated in cement grout has been undertaken on 5 samples. The cone bolt yielding mechanism relies on a tapered cone at the toe of the bolt, (Figure 12) ploughing through the grout to dissipate energy from the loading. Smaller diameter cone bolts encapsulated in cement grout have not been tested.

2.4.1 Testing Program

The cone bolts where encapsulated in two different grout mixes; the first a 0.40 water-cement ratio with strength greater then 40MPa (from grout cylinder testing) and aged for two months to five years, the second was a cement grout and limestone dust mix that achieved 25MPa at 28days (from grout cube testing). The reinforcement systems were trialled with a variety of surface hardware and the simulated discontinuity at 1.0m from the collar.

The steel metallurgical and static mechanical properties of the cone bolt are shown in Table 8. The cone bolt steel conforms with the properties defined by SABS 1408 – 1987.

Figure 12 : Cone bolt

Table 8: Cone Bolt Steel Properties

	Minimum	Maximum	Nominal
Carbon	0.33%	0.4%	0.35%
Managanese	0.78%	0.85%	0.80%
Yield Strength (MPa)	360		400
Ultimate Tensile Strength (MPa)	570		610
Elongation	15%		20%

The test program on the cone bolts is defined in Table 9 and a summary of the results are shown in Table 10..

Table 9: Cone Bolt Test Program

Bolt Number	Loading Mass (kg)	Impact Velocity (m/s)	Input Energy (kJ)	Cement Grout properties	Surface hardware	Collar Tension (kN)
60	2030	5.8	34	25MPa	2 dome plates and rubber plate	60
61	2030	5.85	35	25MPa	Singe dome plate	80
32	2030	5.45	30	>40MPa	2 dome plates and rubber plate	115
41	1980	5.75	33	>40MPa	Singe dome plate	80
35	1890	8.05	61	>40MPa, 5years old	Double dome plate	60

Table 10: Summary of Cone Bolt Results

Bolt Number	Load Time (ms)	Displacement (mm)	Peak Deceleration (g)	Peak Force (kN)	Peak Ejection Velocity (m/s)	Energy Absorbed (kJ)	Proportion of cone movement in separation
60	137	288	-7	157	3.8	32.8	100%
61	120	273	-7.5	167	3.5	35.0	100%
32	73	120	-9.5	209	3.1	19.0	80%
41	69	120	-10	217	2.9	20.5	30%
35	102	312	-10.5	213	5.0	55.6	98%

2.4.2 Summary Cone Bolts

The mechanism of energy dissipation by the cone bolt in high strength (>40MPa) cement grout was a combination of cone movement and plastic deformation of the shaft of the bolt. The plastic deformation of the steel shaft will occur at an elevated yield stress, consistent with the work from Malvar and Crawford (1998). The relative split between the two is dependent on the collar tension applied to the bolt. Generally, high initial tension resulted in greater cone movement but this was not consistent; but at low to no tension there was consistently minimal to no cone movement and only plastic deformation of the shaft of the bolt. The explanation for this mechanism has not be been fully investigated.

The mechanism in the low strength (25MPa) cement and limestone dust grout was cone movement to dissipate the input energy. This occurred at a lower resistive force than that of the cone bolt in high strength grout, and, there was no plastic deformation of the shaft of the bolt. This permitted the later repeat impacts to have the same loading conditions on the surface restraint as the first test. Three tests performed on bolts 60 and 61 showed a slightly lower resistive force for each test; this indicated there was also a frictional component of resistance on the shaft of the cone bolt and not just the cone ploughing through the grout. There appears to be no relationship with collar tension on the ability of the cone to yield through the 25MPa grout.

Cone bolt performance was primarily affected by grout strength with a significant difference in performance between the 25MPa and 40MPa grout; example force-displacement response plots are shown in Figure 13. This means that cone bolts require the selection of a suitable grout to provide a total drive deformation appropriate to the mine requirements.

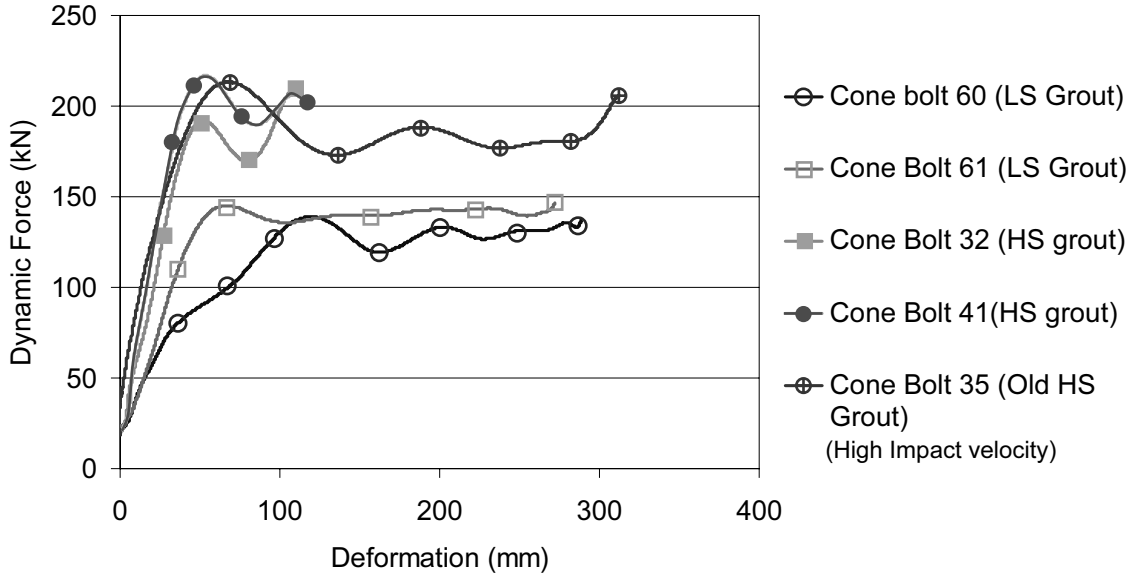

Figure 13: Dynamic force-displacement responses for 22mm cone bolts

2.5 Garford Solid Yielding Bolt

The objectives the test program for this new bolt (Figure 14) was to:

- Statically and dynamically test a prototype version of the bolt and make recommendations for improvements.
- Statically and dynamically test the modified version of the bolt.
- Undertake comparative tests of the bolt in resin and grout to simulate alternative underground conditions.
- Assess displacement of the element under different dynamic conditions.

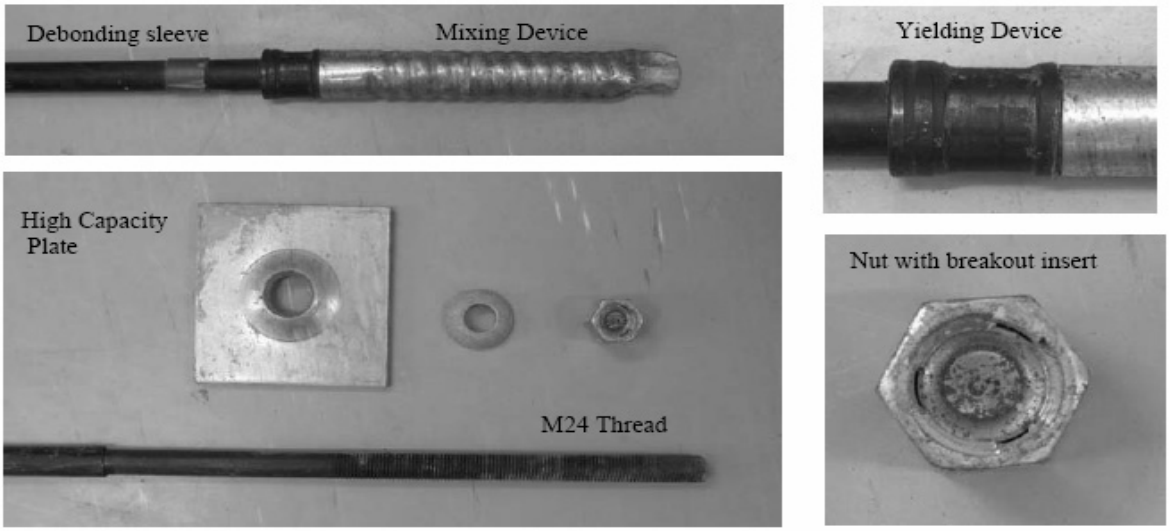

Figure 14: Garford solid yielding bolt

2.5.1 Test program on modified version

The test program had four components:

- Dynamically test the modified version of the bolt cement grouted into thick wall steel pipe of equivalent radial stiffness of 80GPa (Hyett, Bawden and Reichardt, 1992). This simulated the bolt under ideal conditions.
- Development of a simulated bore hole that allowed installation of the bolt by a jumbo with resin into a suitably "rough" borehole, with equivalent radial stiffness of 35GPa. The rough borehole should be similar to a borehole drilled in hard rock. The bolt installed in the rough simulated borehole would then be tested.
- Assess the bolt for effectiveness of resin mixing, encapsulation and damage to the bolt during installation.
- Dynamically test the second version of the bolt installed by a jumbo into the simulated holes, dissect the simulated holes and examine the samples.

Dynamic testing on the bolts and simulated boreholes, simulated a discontinuity at 1.0m from the collar and a nominal 2000kg loading mass on the collar. Due to the robust performance of the Garford bolt, it was possible to undertake multiple loadings on each samples. However, only the first drop results are reported.

2.5.2 Results from test program

The dynamic force-displacement responses are shown in Table 11 and Figure 15 from the first loadings for the Garford solid yielding bolt.

The tests on bolt identified a number of key features;

- When installed in grout and subject to the standard WASM test the bolt had 180mm of displacement with a resistive force of 145kN.
- The bolt behaved slightly differently when encapsulated in resin when compared to encapsulation in cement grout, with slightly shorter displacements.
- It was possible for the bolt to be damaged during installation allowing resin to leak into the yielding mechanism increasing the resistive force and decreasing the displacement, e.g. bolt 97; particularly noticed on the first loading.
- The end stop mechanism worked well maximizing energy absorption capacity of the steel with a cup and cone fracture of the steel bar.

Table 11: Garford solid yielding bolt results

Bolt Number	Load Time (ms)	Displacement (mm)	Peak Deceleration (g)	Peak Force (kN)	Peak Ejection Velocity (m/s)	Energy Absorbed (kJ)	Results
89	98	189	-8.2	182	3.2	27	Bolt in grout idealised performance
90	91.5	197	-8.1	180	2.8	26.5	Bolt in grout idealised performance
97	58	95	-14.8	280	4.1	18	High peak due to resin in the yielding mechanism
98	114	167	-8.6	180	4.7	21.4	Bolt installed in resin by jumbo good performance
99	94	169	-9.7	199	4.0	23.6	Bolt installed in resin by jumbo good performance
100	147	405	-11	240	5.5	53.1	High impact test – end stop mechanism reached and shaft of bolt yields

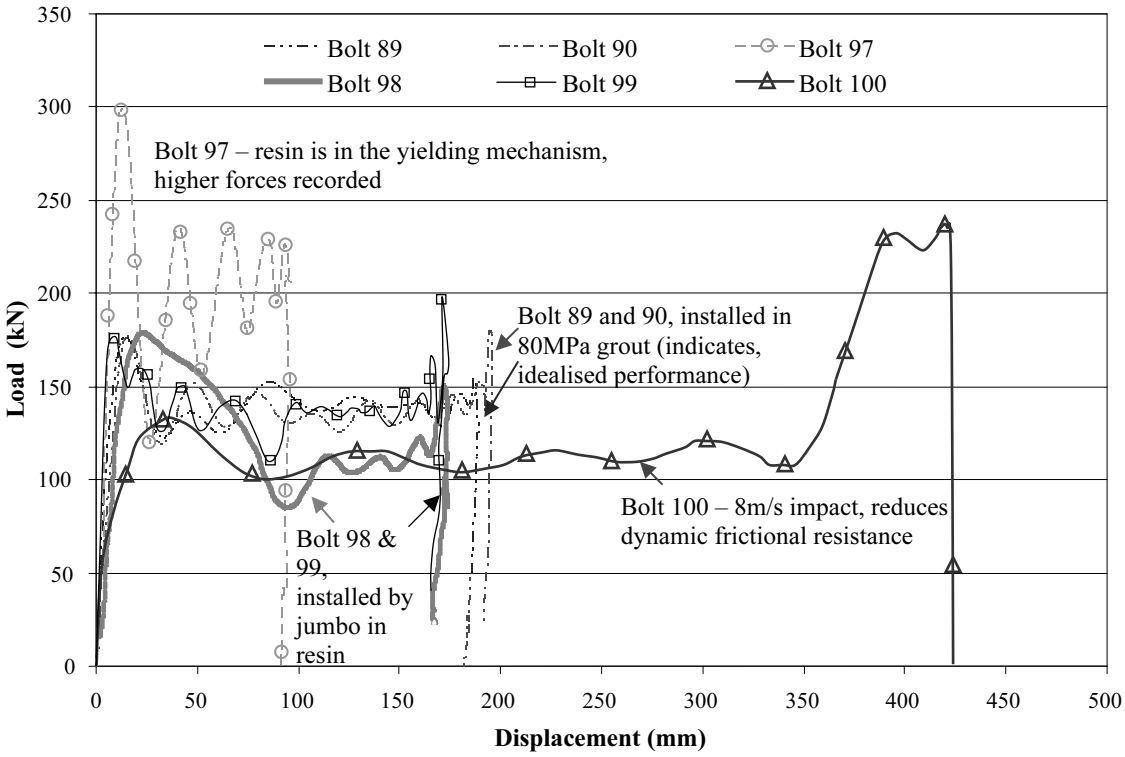

Figure 15 : Dynamic force-displacement responses from Garford solid yielding bolt

2.5.3 Simulated boreholes for jumbo installation of the Garford bolt

The construction of simulated boreholes allowed the testing of reinforcement systems that are sensitive to installation methodology or borehole geometry. The reinforcement system is installed by the equipment that will undertake the task underground and then the complete system can be dynamically tested. A high strength cement grout and basalt aggregate mix was cast about a polystyrene central guide inside of an 80mm internal diameter 100mm outside diameter steel pipe. The required hole was drilled into the high strength grout and basalt aggregate mix by an airleg drill with an appropriately sized bit. The complete unit was pushed into a 150mm hole drilled into the wall of the drive. This allowed the jumbo to install the resin encapsulated bolt into the simulated hole, Figure 16.

Figure 16: Trial bolt installation below simulated boreholes

2.5.4 Dissection of simulated boreholes

The jumbo installed resin encapsulated bolts in the simulated boreholes where dissected (Figure 17) after dynamic loading. The dissection showed;

- the mixing device was very effective, with best encapsulation being achieved by rotating the bolt and slowly pushing the bolt through the entire length of the resin,
- an over-drill allowance of 100mm to 150mm at the end of the hole allowed the resin bag to move to the end of the hole and not wrap around the mixing device,
- A resin length of 240mm between the yielding device on the bolt and the collar sufficient to break the shaft of bolt once the end stop mechanism was reached.

Figure 17: Dissection of toe length from bolt 97

2.5.5 Dependence on loading velocity

The result from the test on bolt 100 (8m/s at impact) indicates a dependence of the dynamical frictional resistance of the steel bar pulling through the yielding device to the velocity of impact. This occured even though the majority of energy consumed was consumed by radial and axial plastic deformation of the bar caused by the yielding device. A change in dynamic friction has been reported by numerous authors across a variety of fields, these include Forrester (1946) in steel, Spurr and Newcomb (1957) for bitumen, and Toro, Goldsby and Tullis (2004) quartz for earthquake faults. The explanation for the process varies depending on the properties of the materials involved. The most important aspect is that the Garford bolt performance exhibits a loading velocity dependence that increased the sliding velocity and decreased the resistance to yield.

The test on bolt 100 also showed that cumulative addition of energy absorbed from several drops leading up to breakage is not necessarily going to be the same as the energy required to break the reinforcement system from a single impact. Bolt 100 absorbed 53kJ with the end-stop mechanism taking significant load while bolts 89 and 90 apparently absorb the same amount of energy on the first two drops without reaching the end stop mechanism. The suggested total energy absorption capability from summing smaller impacts of 65-70kJ from bolts 89, 90 and 99 is shown to be a 20-30% overestimate of the bolts ultimate single loading capacity of 53kJ measured in the test on bolt 100.

This also implies that to be able to determine the true energy absorption of a reinforcement system or support element, the test apparatus must be able to break the reinforcement on the first impact.

3.0 PRACTICAL IMPLICATIONS FROM REINFORCEMENT TESTS

The more a reinforcement system moves during a dynamic loading event, the greater the energy a reinforcement system must be capable of adsorbing due to the additional potential energy input from the “rock” moving into the drive. Yielding systems that allow large displacements due to their softness may also result in excessive fracturing / bulking of the rockmass and have adverse loading of the support system. A soft response from a reinforcing system will also allow higher ejection velocities of the rock into the drive.

Reinforcement systems that are shown to survive multiple loadings should also have a single test with the input energy similar to the sum of the energy absorbed by multiple loadings to assess consistency in behavior across a range of loadings.

Results from the reinforcement tests summarisied in Tables 3, 6, 7, 10, 11 are compiled in the following summary figures. The results are expressed as energy absorbed by the

reinforcement system and separation at the simulated discontinuity (Figure 18), energy absorbed and time to consume the energy from the test (Figure 19), and displacement at the simulated discontinuity and the average dynamic force and displacement, (Figure 20). The figures show increasing energy absorbed with increasing separation at the discontinuity as would be expected from an increase in potential energy from additional displacement of the mass. The increased displacement occurs because of a lower resistive dynamic force from the reinforcement system either from the effect of a yielding system / device or plastic deformation of the steel bar.

Relationships between displacement and 'ejection' velocity primarily show that high displacement systems will yield with a higher velocity. This implies an improved survivability for high eject velocity events. However it is important that the stiffness and capacity of the support system and reinforcement system are well matched to ensure survival of the overall scheme.

The circled results on the three figures represent samples that broke during testing.

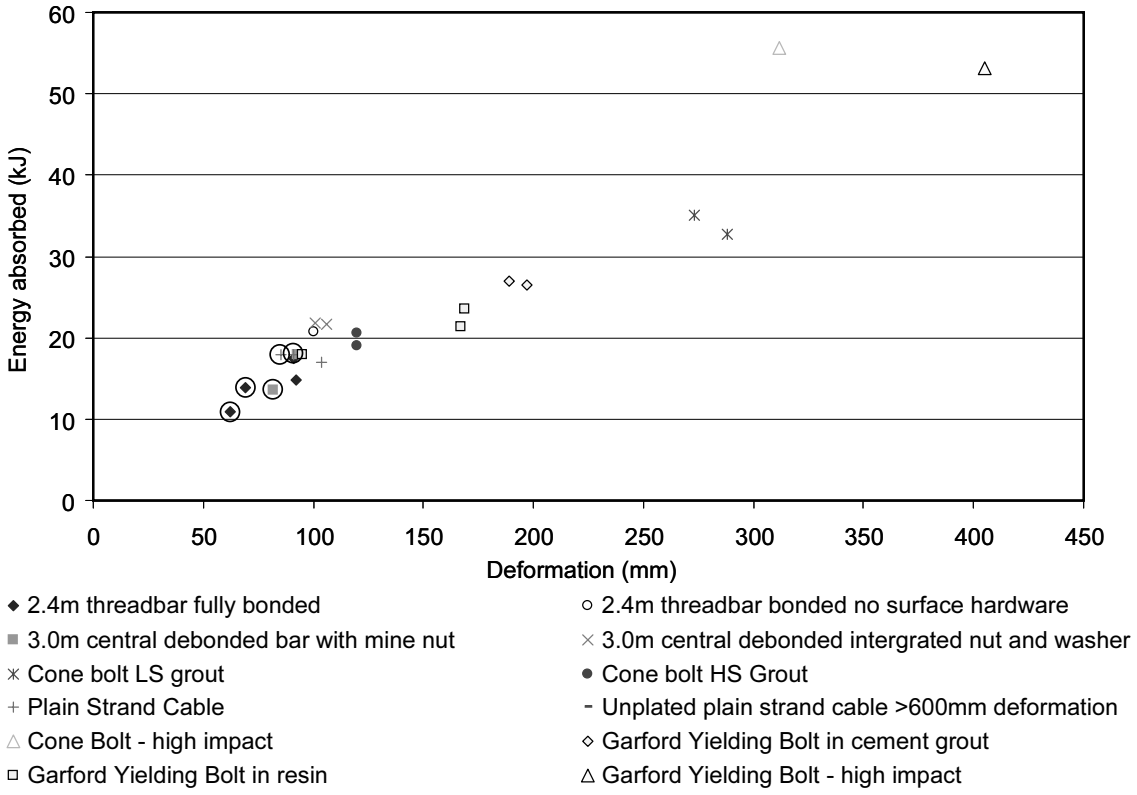

Figure 18: Energy absorbed by reinforcement systems with deformation for WASM Dynamic testing

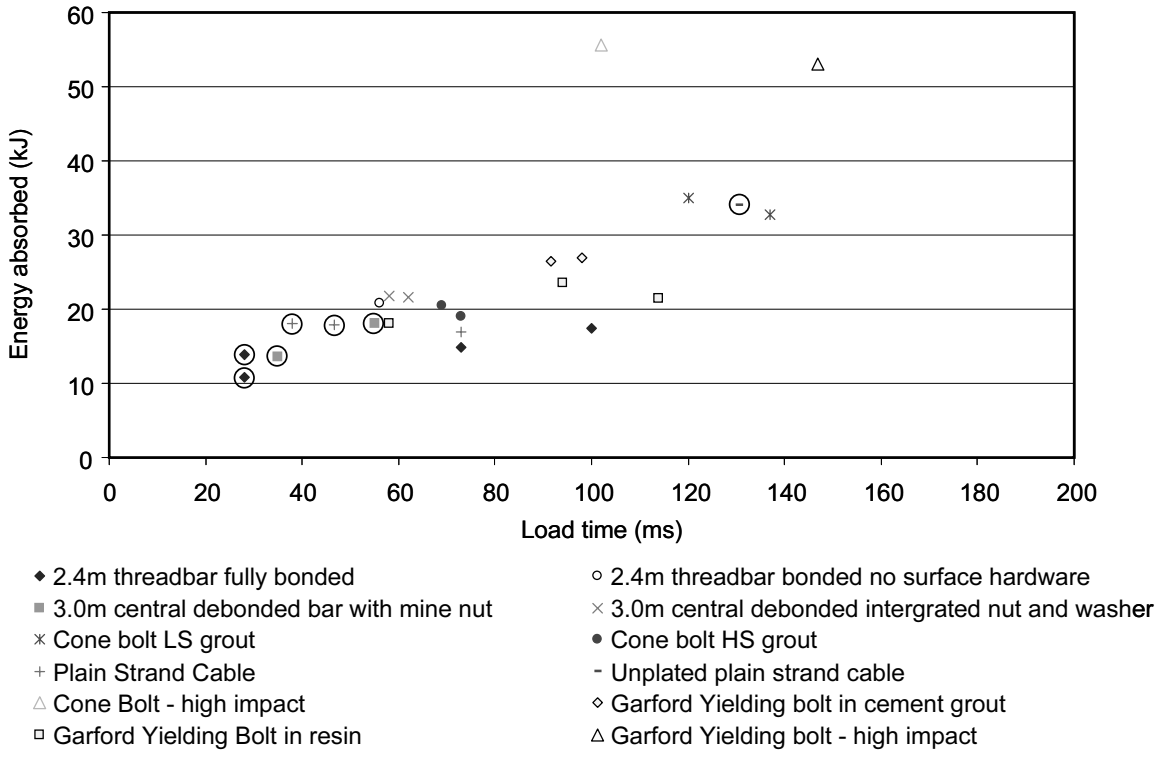

Figure 19: Energy absorbed by reinforcement systems with loading time for WASM Dynamic testing

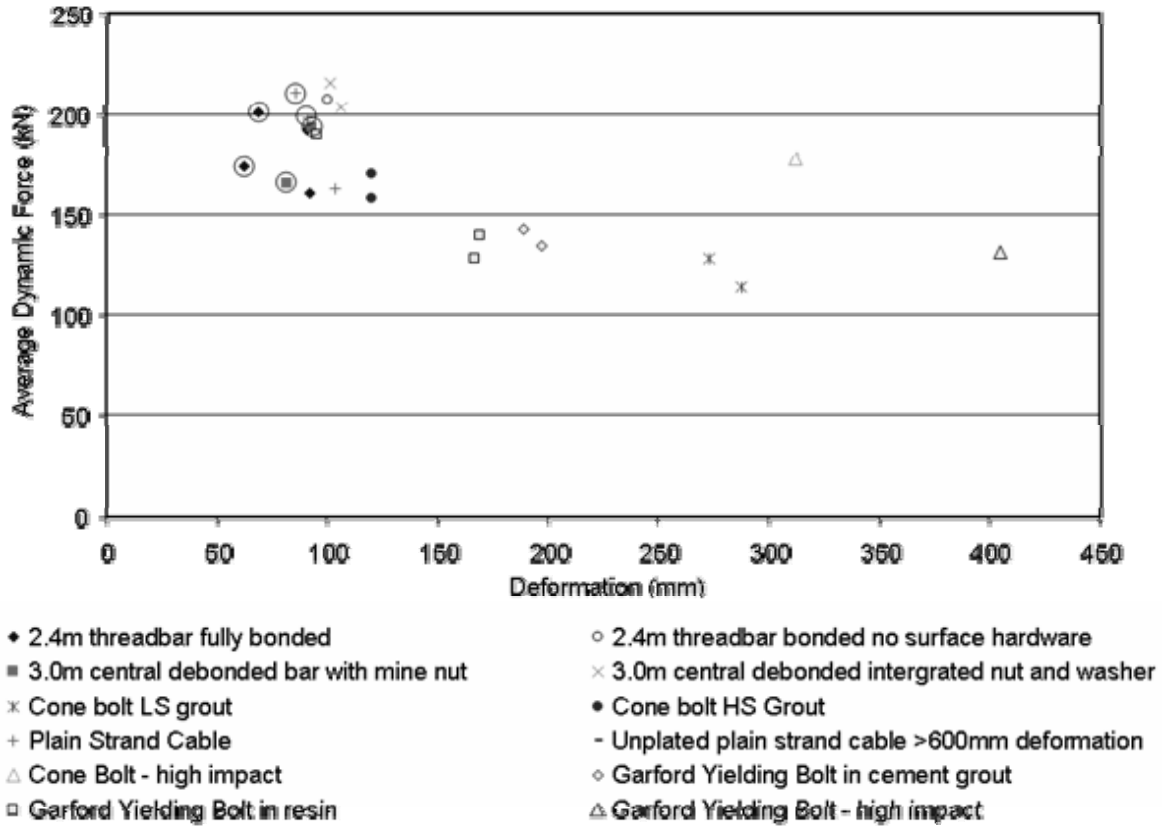

Figure 20: Average dynamic force and deformation from WASM dynamic testing

4.0 CONCLUDING REMARKS

The WASM Dynamic Test Facility has been used to quantify the performance of various reinforcement systems in use and with potential for use in the Australian mining industry.

Testing of reinforcement systems at the WASM Dynamic Test Facility is undertaken under axial loading conditions. The testing methodology and facility provides repeatable results. The calculated dynamic force-displacement responses, energy absorbed and duration of loading for the reinforcement systems are only applicable for the load and method of load application in the WASM Dynamic Test Facility.

The double embedment testing methodology is shown to be important in ;

- simulating the bonding that occurs between the reinforcement element, the locking medium and the side of the borehole and hence correctly simulating how the reinforcement system behaves in response to block ejection, and
- testing of surface hardware with the reinforcing element for understanding the capacity of the reinforcement system.

The test program identified ;

- the 2.0m critical embedment length for 15.2mm plain strand cable to ensure breakage is the same for static and dynamic axial loading; otherwise slip occurs.

- the plating of plain strand cable bolts maximises the capacity of the strand.
- the critical loading requirement to break threadbar occurs when the plastic deformation of the steel is faster than the growth of new fractures in the grout and the delayed development of a "debonding" surface at the simulated discontinuity.
- An increase in the yield strength of the steel for dynamic loading compared to the quasi-static yield strength due to the strain rate, which is consistent Malvar and Crawford (1998).
- a strong correlation of cone bolt performance with the strength, and possibly stiffness, of the encapsulation media and a secondary dependence on the installed tension, particularly when installed in high strength material.
- the Garford solid yielding bolt can be installed in either a cement or resin grout and function as designed. The engineered yielding device provides a more repeatable energy absorption mechanism than an element moving through a failing material.
- the Garford solid yielding mechanism bolt indicates a dependence on the loading velocity due to the frictional mechanism
- a test facility must have sufficient energy input to break a reinforcement system on the first loading in order to predict the ultimate capacity of the system compared with summing a series of separate loadings.

Ongoing research is being conducted on friction stabilisers. The research to date has identified high variability in performance compared with other reinforcement systems.

The WASM facility has also tested support elements such as chain link mesh made from high tensile strength wire and standard welded mesh products. A program of dynamic testing of fibrecrete panels has commenced. Player et al. (2008) describe the static and dynamic results from tests on support elements.

Higher impact loading conditions, or shear loading may result at underground openings due to a dynamic shear / violent rock failure event. Such loading conditions could change the performance of the reinforcement system.

Companies using the results must make their own determination on underground installation quality and the suitability of the loading mechanism, potential energy release from a seismic source as to how the performance of their reinforcement system would change at a particular site presented herein.

ACKNOWLEDGEMENTS

The writers would like to thank the sponsoring organisations of MERIWA Project M349 and M349A – Dynamic Testing of Reinforcement and Support Systems, Minerals and Energy Research Institute of Western Australia; namely, Barrick – Kanowna Belle, Strata Control Systems, DSI, Atlas Copco, BHP Nickel West, Geobrugg, Newmont Gold, Harmony Gold, Kalgoorlie Consolidated Gold Mines, Lightning Nickel, Onesteel and the WA government through MERIWA.

References

Anon 2006, *Strata Control Systems Product Catalogue Version 4*, Sydney.

Brown, ET, 2004, 'The Dynamic Environment of Ground Support and Reinforcement'. *Ground Support in Mining and Underground Construction*, eds. Villaescusa and Potvin, pp3-16, Balkema: Leiden.

Forrester, PG, 1946, 'Kinetic Friction in or Near the Boundary Region. II. The Influence of Sliding Velocity and Other Variables on Kinetic Friction in or Near the Boundary Region'. *Proceedings of the Royal Society of London. Series A, Mathematical and Physical Sciences,* 187**,** pp439-463.

Malvar, LJ and JE Crawford, 1998, 'Dynamic increase factors for steel reinforcing bars', in *28th Department of Defence Explosive Safety Board Seminar*, Orlando, Florida, August 1998.

Player, JR, E Morton, AG Thompson, and E Villaescusa, 2008, 'Static and Dynamic Testing of Steel Wire Mesh for Mining Applications of Rock Surface Support ', *Ground Support in Mining and Underground Construction.* Capetown.

Player, JR, AG. Thompson and E. Villaescusa 2004. 'Dynamic Testing of Rock Reinforcement using the Momentum Transfer Concept'. *Ground Support in Mining and Underground Construction*, eds. Villaescusa and Potvin, pp327-340, Balkema: Leiden.

Player, JR, E Villaescusa, and Thompson, AG 2005, 'An Examination of Dynamic Test Facilities', Chapter 9 *Advanced Geomechanics in Mines*, ed. E Potvin, Australian Centre for Geomechanics, Perth.

Thompson, AG, JR. Player and E. Villaescusa 2004. 'Simulation and analysis of dynamically loaded reinforcement systems'. *Ground Support in Mining and Underground Construction*, eds. Villaescusa and Potvin, pp341-358, Balkema:Leiden.

Hutchins, WR, Bywater, S, Thompson, AG and Windsor, CR 1990. 'A Versatile Grouted Cable Dowel Reinforcing System for Rock'. *The AusIMM Proceedings*, No. 1, pp25-29.

Hyett, A, Bawden, W & Reichardt, R 1992, 'The Effect of Rockmass Confinement on the Bond Strength of Fully Grouted Cable Bolts', *International Journal of Rock Mechanics, Mining Science, and Geomechanics Abstracts,* vol. 29, pp503-24.

Spurr, RT, and Newcomb, TP, 1957 'The Variation of Friction with Velocity'. *Proceeding of the Physics Society. Section B,* 70**,** pp198-200.

Toro, GD, Goldsby, DL, and Tullis, T E, 2004 'Friction Falls towards Zero in Quartz Rock as Slip Velocity Approaches Seismic Rates'. *Nature,* 427**,** pp436-439.